

Paper submitted for publication in an IEEE journal.

© 2021 IEEE. Personal use of this material is permitted. Permission from IEEE must be obtained for all other uses, in any current or future media, including reprinting/republishing this material for advertising or promotional purposes, creating new collective works, for resale or redistribution to servers or lists, or reuse of any copyrighted component of this work in other works.

arXiv:2111.04678v1 [cs.IT] 8 Nov 2021

Joint Optimization of Uplink Power and Computational Resources in Mobile Edge Computing-Enabled Cell-Free Massive MIMO

Giovanni Interdonato and Stefano Buzzi

Abstract

The coupling of cell-free massive MIMO (CF-mMIMO) with Mobile Edge Computing (MEC) is investigated in this paper. A MEC-enabled CF-mMIMO architecture implementing a distributed user-centric approach both from the radio and the computational resource allocation perspective is proposed. An optimization problem for the joint allocation of uplink powers and remote computational resources is formulated, aimed at minimizing the total uplink power consumption under power budget and latency constraints, while simultaneously maximizing the minimum SE throughout the network. In order to efficiently solve such a challenging non-convex problem, an iterative algorithm based on sequential convex programming is proposed, along with two approaches to priory assess the problem feasibility. Finally, a detailed performance comparison between the proposed MEC-enabled CF-mMIMO architecture and its cellular counterpart is provided. Numerical results reveal the effectiveness of the proposed joint optimization problem, and the natural suitability of CF-mMIMO in supporting computation-offloading applications with benefits over users' transmit power and energy consumption, the offloading latency experienced, and the total amount of allocated remote computational resources.

Index Terms

Cell-free massive MIMO, computation offloading, power minimization, mobile edge computing, convex optimization.

This paper was supported by the Italian Ministry of Education University and Research (MIUR) Project “Dipartimenti di Eccellenza 2018-2022” and by the MIUR PRIN 2017 Project “LiquidEdge”. An excerpt of this article has been submitted to the 2022 IEEE International Conference on Communications (ICC) [1]. The authors are with the Department of Electrical and Information Engineering (DIEI) of the University of Cassino and Southern Latium, 03043 Cassino, Italy (e-mail: giovanni.interdonato@unicas.it, buzzi@unicas.it); they are also with the Consorzio Nazionale Interuniversitario per le Telecomunicazioni (CNIT), 43124, Parma, Italy.

I. INTRODUCTION

The recent evolution of wireless networks has been characterized by an impressive growth not only of the amount of conveyed data traffic, but also of computationally-intensive applications with strict latency requirements for mobile devices. Applications such as online gaming, augmented reality and video image processing not only request extreme broadband connections, but also a considerable amount of computational power at the mobile devices. A possible approach to indirectly increase the computing capabilities of the devices and prolong their battery lifetime is to (either fully or partially) delegate their computational tasks to the network, specifically to network entities, known as *network edge servers*¹, in charge of collecting, processing and feeding data back to the users in a centralized fashion. This approach is known as *mobile edge computing* (MEC) or mobile-edge computation offloading [2]–[6]. Similarly, additional computing resources may be made available at the core network via cloud computing, as in the case of the centralized architecture C-RAN (Cloud-Radio Access Network) [7], [8]. C-RAN is also a potential architecture to implement cell-free massive multiple-input multiple-output (CF-mMIMO) systems [9], [10], a recently introduced evolution of traditional multi-cell massive MIMO systems [11]–[13]. Cell-free massive MIMO is a technology based on the use of several distributed low-complexity access points (APs), equipped with few antennas, that jointly serve the active users in their coverage area. It inherits all the outstanding features of co-located massive MIMO [14], [15], such as nearly-optimal linear signal processing, predictable accurate performance, and simplified resource allocation and channel estimation, while providing additional key ingredients to theoretically achieve unprecedented levels of uniform data rates and ubiquitous connectivity: macro-diversity gain, inter-cell interference mitigation, and user proximity. Moreover, it is also amenable to scalable user-centric implementations [16]–[18].

In this paper, we investigate the promising marriage between CF-mMIMO and MEC. CF-mMIMO, thanks to its dense distributed topology and user-centric architecture, can greatly facilitate the computation offloading, by enabling mobile devices to delegate either all or part of their computational tasks to multiple APs, each of which may be equipped with an edge server. Moreover, the central processing unit (CPU) of a CF-mMIMO system, which is generally equipped with a more powerful server, may serve as a mobile cloud computing, to give, in

¹The edge servers are network entities figuratively placed at the *edge* of the cellular access network, that is between the radio access network and the core network.

turn, computation offloading support to the single APs. User proximity and the macro-diversity can significantly reduce the delay due to the computation offloading, and the user's power consumption, while fulfilling stricter latency requirements. Moreover, the user-centric approach ensures uniform spectral efficiency (SE) for every user, and thereby the access to the remote computational resources can be indiscriminately granted to everyone. On the other hand, the amount of computational tasks that each user can offload to the network clearly depends on its uplink SE, hence determined by users' uplink transmit powers. This coupling calls out for a joint optimization of radio and computational resources, which is the main subject of this study.

A. *Related Works*

Most works on MEC optimize the interplay between the amount of computational tasks to offload, the latency due to the offloading operation, and the energy consumption of mobile devices. For instance, the energy consumption under delay constraints is minimized in [19], [20], while in [21] the remote computational time is minimized under energy consumption constraints.

First studies on MEC assumed simplified system models by considering either single-user systems [22]–[24] or interference-free multi-user systems [19], [25]. Some of these works considered a binary model for the computation offloading, wherein each device either offloads the entire amount of its computational tasks, or execute them locally [19], [22]. Other studies, alternatively, assumed a more general partial computation offloading [23], [25]. An integrated framework for computation offloading and interference management in wireless cellular networks with MEC was proposed in [26]. All these works assumed single-antenna mobile devices.

More recently, MEC has been studied in conjunction with MIMO technologies. As an example, [4] considers a multi-cell MIMO system served by an edge server in a centralized fashion (e.g., C-RAN architecture), and formulates a total energy minimization problem while meeting the latency and minimum rate constraints. Such non-convex problem is solved through successive convex approximation (SCA). Similarly, the MEC solution proposed in [27] focuses on iteratively minimizing the maximum latency of all the devices in a network with MIMO C-RAN architecture. Additionally, [28] addresses the energy minimization problem accounting for imperfect channel state information (CSI) in a single-cell MIMO system. In [29], a successive inner convexification framework to minimize the total transmit power of the devices under latency constraints is proposed; the obtained solution is compared to a supervised deep learning approach, as less computationally demanding and thus more suitable for real-time Internet-of-Things applications.

Several authors have also examined the coupling between MEC and massive MIMO. The paper [30] proposes a low-complexity algorithm, based on alternating optimization, to jointly optimize the radio and computing resources for a massive MIMO-enabled heterogeneous network (HetNet) with MEC. Similarly, [20], [31] presented the effectiveness of employing massive MIMO for MEC, under zero-forcing combining, aiming at minimizing the maximum delay for offloading and computing among the devices. The paper [32], instead, considers a massive MIMO system operating at the millimeter-wave frequency bands underlying traditional wireless local area networks with MEC. The main common conclusion of these works is that multiple users can simultaneously offload their computational tasks by leveraging the additional degrees-of-freedom provided by massive MIMO, and the offloading efficiency, as well as the energy saving of the mobile devices, grows with the number of antennas of the massive MIMO BS.

Finally, the performance of CF-mMIMO with MEC functionalities has been recently explored in [33]. Specifically, this work studies a joint radio and computational resources allocation using queuing theory and stochastic geometry, hence considering a random computation latency model, a dynamic number of edge computing servers and of offloaded tasks/devices. The system model in [33] consists of APs equipped with independent MEC servers, and a CPU with a central MEC server (CS), and each device performs offloading either to the CS or to one of its serving APs, with some successful computing probability, which affects the total energy consumption. Hence, such a system implements a cell-free user-centric approach from the radio resource allocation viewpoint, but it does not from the MEC perspective. Following on this track, we explore in this paper the potential benefits of jointly optimizing radio and computational resources in a CF-mMIMO system with user-centric MEC approach.

B. Contribution

Our technical contribution can be summarized as follows.

- We propose a MEC-enabled CF-mMIMO architecture implementing a user-centric approach both from the radio and the computational resource allocation perspective. Unlike prior studies investigating computation-offloading implementations in distributed networks but operating in a centralized fashion [29], [30], [33], our model considers that users' computational tasks can be executed in a distributed fashion both at the MEC servers of the user-centric cluster and at the cloud CPU.
- We formulate an optimization problem for jointly allocating users' transmit powers and the remote computational resources for offloading. Similarly to prior works such as [4], [30],

we aim at minimizing the total uplink power consumption under power budget and latency constraint. However, our formulation simultaneously maximizes the minimum SE throughout the network. Such a max-min fairness approach can significantly reduce the transmission latency and user's power consumption, while fulfilling stricter latency requirements.

- We devise an SCA algorithm for efficiently solving our optimization problem. The proposed SCA algorithm has some similarities with that in [30], but additionally includes: (i) the user-centric cooperation clustering framework; (ii) a distributed allocation of the computational resources; (iii) a general formulation for any combining scheme.
- Two novel approaches to assess the feasibility of the considered optimization problem are presented. A first approach gives a rough assessment on the problem feasibility, but it permits to speed up the convergence of the proposed SCA algorithm by giving in input a set of (very likely) feasible uplink powers. A second approach provides a rigorous assessment on the problem feasibility, at the price of higher computational complexity.
- We compare the proposed MEC-enabled CF-mMIMO architecture with its cellular counterpart. To do this, we reformulate and solve the joint radio and computational resource allocation problem also for a co-located massive MIMO system. In our numerical results, we will observe performance improvements for the MEC-enabled CF-mMIMO deployment in terms of: (i) users' transmit power and energy consumption, (ii) users' transmission latency, and (iii) amount of allocated remote computational resources.
- A further insight about the effectiveness of the proposed joint optimization of uplink power and computational resources is finally provided, by evaluating the interplay between uplink power, SE, allocated remote computational resources, and effective MEC offloading latency.

II. SYSTEM MODEL

We consider a CF-mMIMO system operating in time-division duplexing (TDD) mode, and at sub-6 GHz frequency bands. A set of L APs, equipped with M antennas each, are geographically distributed and connected through a fronthaul network to a CPU. The APs coherently serve K single-antenna users in the same time-frequency resources, with $LM \gg K$.

The conventional block-fading channel model is considered, and let τ_c denote the channel coherence block length. In TDD mode, each coherence block accommodates uplink training, uplink and downlink data transmission, such that $\tau_c = \tau_p + \tau_u + \tau_d$, where τ_p , τ_u and τ_d are respectively the training duration, the uplink and the downlink data transmission duration, respectively.

Borrowing the notation of [18], the channel between the k -th user and the l -th AP is denoted by the M -dimensional vector \mathbf{h}_{lk} , with $\mathbf{h}_{lk} \sim \mathcal{CN}(\mathbf{0}, \mathbf{R}_{lk})$, and $\mathbf{R}_{lk} \in \mathbb{C}^{M \times M}$ being the spatial correlation matrix. The corresponding large-scale fading coefficient is defined as $\beta_{lk} = \text{tr}(\mathbf{R}_{lk})/M$. The channel between the k -th user and all the APs in the system is obtained by stacking the channel vectors \mathbf{h}_{lk} , $\forall l$ as $\mathbf{h}_k = [\mathbf{h}_{1k}^T \cdots \mathbf{h}_{Lk}^T]^T \in \mathbb{C}^{ML}$. The channel vectors of different APs are reasonably assumed to be independently distributed. As a consequence, we have $\mathbf{h}_k \sim \mathcal{CN}(\mathbf{0}, \mathbf{R}_k)$, where $\mathbf{R}_k = \text{diag}(\mathbf{R}_{1k}, \dots, \mathbf{R}_{Lk}) \in \mathbb{C}^{ML \times ML}$ is the block-diagonal spatial correlation matrix of user k .

A. Centralized Uplink Training

During the uplink training all the K users synchronously send a pre-determined pilot sequence whose length in samples is denoted by τ_p . The pilot sequences are drawn by a set of τ_p orthonormal vectors. Specifically, $\sqrt{\tau_p} \boldsymbol{\varphi}_k \in \mathbb{C}^{\tau_p}$ denotes the pilot sent by the k -th user, with $\|\boldsymbol{\varphi}_k\| = 1$. Whenever K is larger than τ_p , the same pilot must be assigned to more than one user. Assuming that the channel estimation is performed by the CPU, in each coherence interval, each AP needs to send its received pilot signal to the CPU. The pilot signal observed by AP l is

$$\mathbf{Y}_{p,l} = \sum_{j=1}^K \sqrt{\tau_p p_{p,j}} \mathbf{h}_{lj} \boldsymbol{\varphi}_j^T + \boldsymbol{\Omega}_{p,l} \in \mathbb{C}^{M \times \tau_p},$$

where $p_{p,j}$ is the transmit power of the uplink pilot symbol, and $\boldsymbol{\Omega}_{p,l}$ is a matrix of additive noise whose elements are independently distributed as $\mathcal{CN}(0, \sigma^2)$. To estimate the channel of user k , the l -th AP projects $\mathbf{Y}_{p,l}$ along the k -th pilot sequence, which yields:

$$\mathbf{y}_{lk}^p = \mathbf{Y}_{p,l} \boldsymbol{\varphi}_k^* = \sqrt{\tau_p p_{p,k}} \mathbf{h}_{lk} + \sum_{j \neq k}^K \sqrt{\tau_p p_{p,j}} \mathbf{h}_{lj} \boldsymbol{\varphi}_j^T \boldsymbol{\varphi}_k^* + \boldsymbol{\Omega}_{p,l} \boldsymbol{\varphi}_k^* \in \mathbb{C}^M.$$

The vector \mathbf{y}_{lk}^p is then sent to the CPU which, upon a prior knowledge of the channel correlation matrices, takes care of performing linear minimum-mean square error (MMSE) estimation of the k -th user channel \mathbf{h}_{lk} through the processing $\hat{\mathbf{h}}_{lk} = \sqrt{\tau_p p_{p,k}} \mathbf{R}_{lk} \boldsymbol{\Psi}_{lk}^{-1} \mathbf{y}_{lk}^p$, where $\boldsymbol{\Psi}_{lk}$ is the covariance matrix of \mathbf{y}_{lk}^p . The estimation error is independent of the estimate, and given by $\tilde{\mathbf{h}}_{lk} = \mathbf{h}_{lk} - \hat{\mathbf{h}}_{lk}$. It is distributed as $\tilde{\mathbf{h}}_{lk} \sim \mathcal{CN}(\mathbf{0}, \mathbf{C}_{lk})$, with $\mathbf{C}_{lk} = \mathbb{E} \left\{ \tilde{\mathbf{h}}_{lk} \tilde{\mathbf{h}}_{lk}^H \right\} = \mathbf{R}_{lk} - \tau_p p_{p,k} \mathbf{R}_{lk} \boldsymbol{\Psi}_{lk}^{-1} \mathbf{R}_{lk}$. Hence, all the channel estimates for a specific user k are collected in the vector $\hat{\mathbf{h}}_k = [\hat{\mathbf{h}}_{1k}^T \cdots \hat{\mathbf{h}}_{Lk}^T]^T$. Accordingly, it holds $\tilde{\mathbf{h}}_k = \mathbf{h}_k - \hat{\mathbf{h}}_k \sim \mathcal{CN}(\mathbf{0}, \mathbf{C}_k)$, with $\mathbf{C}_k = \text{diag}(\mathbf{C}_{1k}, \dots, \mathbf{C}_{Lk})$.

B. User-Centric Uplink Data Transmission

In a practical and scalable user-centric implementation, each user is not served by all the APs in the network, but rather by a limited number of APs selected among those ensuring

the best channel conditions. This AP-user association is performed by the CPU, and can be mathematically handled by a set of auxiliary diagonal matrices $\mathbf{D}_{lk} \in \mathbb{C}^{M \times M}, \forall l, \forall k$. Specifically, $\mathbf{D}_{lk} = \mathbf{I}_M$, if AP l serves user k , and $\mathbf{D}_{lk} = \mathbf{0}_M$, if AP l does not serve user k . This user-centric approach has two main implications: (i) the estimates needed at the CPU to design the receive combining vectors are limited to $\mathbf{D}_k \hat{\mathbf{h}}_k$, with $\mathbf{D}_k = \text{diag}(\mathbf{D}_{1k}, \dots, \mathbf{D}_{Lk})$ being a block-diagonal matrix; (ii) the uplink signals needed at the CPU for data decoding are limited to $\mathbf{D}_k \mathbf{y}$, with \mathbf{y} being the vector collecting the uplink data signals sent by all the APs to the CPU. Let \hat{s}_k be the estimate of the transmitted data symbol s_k , computed by the CPU through the processing

$$\hat{s}_k = \sum_{l=1}^L \hat{s}_{lk} = \sum_{l=1}^L \mathbf{v}_{lk}^H \mathbf{D}_{lk} \mathbf{y}_l = \mathbf{v}_k^H \mathbf{D}_k \mathbf{y}, \quad (1)$$

where $\mathbf{v}_{lk} \in \mathbb{C}^M$ is the receive combining vector intended for the link between AP l and user k , and $\mathbf{v}_k = [\mathbf{v}_{1k}^T \dots \mathbf{v}_{Lk}^T]^T$. The uplink data signal received by AP l is $\mathbf{y}_l = \sum_{i=1}^K \mathbf{h}_{li} s_i + \mathbf{n}_l$, with $\mathbb{E}\{|s_i|^2\} = p_i, \forall i$, and $\mathbf{n}_l \sim \mathcal{CN}(0, \sigma^2 \mathbf{I}_M)$ being the additive noise vector. While, $\mathbf{y} = [\mathbf{y}_1^T \dots \mathbf{y}_L^T]^T \in \mathbb{C}^{ML}$. Hence, eq. (1) can be rewritten as

$$\hat{s}_k = \mathbf{v}_k^H \mathbf{D}_k \hat{\mathbf{h}}_k s_k + \mathbf{v}_k^H \mathbf{D}_k \tilde{\mathbf{h}}_k s_k + \sum_{i \neq k}^K \mathbf{v}_k^H \mathbf{D}_k \hat{\mathbf{h}}_i s_i + \mathbf{v}_k^H \mathbf{D}_k \mathbf{n}, \quad (2)$$

with $\mathbf{n} = [\mathbf{n}_1^T \dots \mathbf{n}_L^T]^T \in \mathbb{C}^{ML}$ being the collective noise vector. The first term in (2) represents the desired signal over the known partially estimated channel, the second term represents the self-interference due to the (unknown) channel estimation error, the third term is the multi-user interference, and, lastly, the fourth term is the noise. An achievable uplink SE for user k , with centralized operation, is well-known to be obtained by treating the last three terms as uncorrelated noise at the receiver:

$$\overline{\text{SE}}_k = \frac{\tau_u}{\tau_c} \mathbb{E} \{ \log_2(1 + \text{SINR}_k) \}, \quad \text{bit/s/Hz} \quad (3)$$

where

$$\text{SINR}_k = \frac{p_k |\mathbf{v}_k^H \mathbf{D}_k \hat{\mathbf{h}}_k|^2}{\sum_{i \neq k}^K p_i |\mathbf{v}_k^H \mathbf{D}_k \hat{\mathbf{h}}_i|^2 + \mathbf{v}_k^H \mathbf{Z}_k \mathbf{v}_k + \sigma^2 \|\mathbf{D}_k \mathbf{v}_k\|^2} \quad (4)$$

with $\mathbf{Z}_k = \sum_{i=1}^K p_i \mathbf{D}_k \mathbf{C}_i \mathbf{D}_k$. This achievable SE holds for any combining scheme and arbitrary correlated fading channels, and accounts for user-centric data detection, channel estimation error, pilot contamination and estimation overhead.

As to the collective combining vector \mathbf{v}_k , we will adopt, with no loss of generality, the so-called Partial MMSE (P-MMSE) combining [18]. This scheme reduces the computational complexity (which becomes independent of K) by taking into account only the most interference

contributions caused by the other users located in its vicinity, and which are presumably served by partially the same subset of APs. Hence, for an arbitrary user k , P-MMSE considers only the interference contributions caused by the users whose indices are in the set $\mathcal{S}_k = \{i : \mathbf{D}_k \mathbf{D}_i \neq \mathbf{0}_{LM}\}$. The collective P-MMSE combining vector is thus given by

$$\mathbf{v}_k^{\text{P-MMSE}} = p_k \left(\sum_{i \in \mathcal{S}_k} p_i \mathbf{D}_k \hat{\mathbf{h}}_i \hat{\mathbf{h}}_i^H \mathbf{D}_k + \mathbf{Z}_{\mathcal{S}_k} + \sigma^2 \mathbf{I}_{LM} \right)^{-1} \mathbf{D}_k \hat{\mathbf{h}}_k, \quad (5)$$

where $\mathbf{Z}_{\mathcal{S}_k} = \sum_{i \in \mathcal{S}_k} p_i \mathbf{D}_k \mathbf{C}_i \mathbf{D}_k$.

III. COMPUTATION-OFFLOADING AND LATENCY MODEL

We assume that both the APs and the CPU offer computational facility to the user terminals. Each user has a set of computational tasks to process and possibly to offload to the MEC servers of its serving APs and/or to the cloud CPU. We assume that user k needs to execute w_k CPU cycles over b_k computation bits, and within a maximum tolerable latency \mathcal{L}_k . AP l has a computational capability of f_l^{AP} CPU cycles per second (computational rate). While, the cloud CPU can execute up to f^{CPU} instructions per second. The fractions of computational resources assigned to user k by its serving AP l and the CPU are denoted by $f_{l,k}^{\text{AP}}$ and f_k^{CPU} , respectively. Hence, it holds

$$\sum_{k=1}^K f_k^{\text{CPU}} \leq f^{\text{CPU}}, \quad \text{and} \quad \sum_{k \in \mathcal{K}_l} f_{l,k}^{\text{AP}} \leq f_l^{\text{AP}}, \quad \forall l,$$

where \mathcal{K}_l is the set including the indices of the users served by AP l . Let f_k be the overall computational resources assigned to user k , given by $f_k = f_k^{\text{CPU}} + \sum_{l \in \mathcal{M}_k} f_{l,k}^{\text{AP}}$, with \mathcal{M}_k being the set including the indices of the APs serving user k . Then, w_k/f_k represents the computational time needed to execute w_k CPU cycles at the APs and the cloud CPU (*computational latency*). While, the amount b_k/R_k is the time needed to transmit b_k bits to the APs (*transmission latency*), over the wireless channel supporting a rate $R_k = B \times \text{SE}_k$, with B being the transmission bandwidth and SE_k being the instantaneous SE, i.e., the value attained by (3) with no expectation. Lastly, an additional latency contribution (*fronthaul latency*) is due to the forwarding of the b_k bits from all the APs in the set \mathcal{M}_k to the cloud CPU, over the fronthaul network, which, assuming synchronous transmission across the APs, amounts to $2b_k M \xi / C_{\text{FH}}$, where ξ denotes the number of bits used to quantize both real and imaginary parts of the uplink data signal \mathbf{y} , and C_{FH} is the fronthaul capacity of the link between any AP and the cloud CPU, expressed in bit/s. Hence, the computational offloading must fulfill the following latency constraint [29]

$$\frac{b_k}{R_k} + \frac{w_k}{f_k} + \frac{2b_k M \xi}{C_{\text{FH}}} \leq \mathcal{L}_k, \quad \forall k, \quad (6)$$

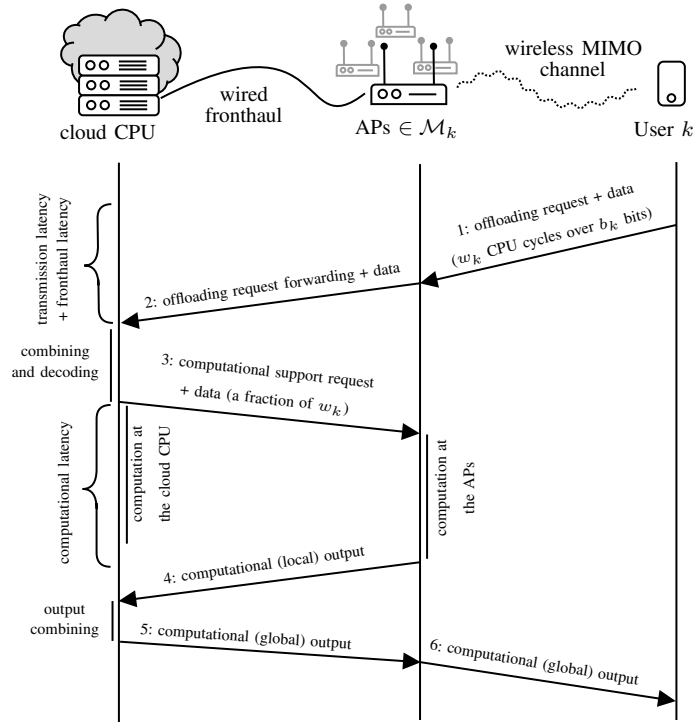


Fig. 1. Signalling diagram describing the computational offloading process for an arbitrary user k . In this example, the computational offloading occurs both at the cloud CPU and the serving APs.

where we assume that \mathcal{L}_k includes any delay related to the signalling between AP and cloud CPU, and the time needed to send the computational output back to the user. Fig. 1 illustrates the signalling diagram of the computational offloading process for an arbitrary user k . As a first step, user k sends a *computational offloading request* followed by the symbols encoding the program to be executed remotely. Then, all the APs serving user k , that is the APs in the set \mathcal{M}_k , forward these uplink signals, over the fronthaul network, to the cloud CPU for centralized receive combining and data decoding. The cloud CPU, according to its available computational resources, executes the offloaded computational task either totally or partially. In the latter case, the CPU sends to the APs in the set \mathcal{M}_k a *computational support request* accompanied by the *batch jobs* (a fraction of the w_k CPU cycles) to be executed in a distributed fashion.² The allocation of the computational resources between cloud CPU and APs is subject to optimization whose characterization is detailed in the next section. Once received the computational output of each batch job from the APs, the cloud CPU sends the combined computational output back to the APs in the set \mathcal{M}_k , which finally perform a joint data transmission to user k .

²We assume that users' programs can be divided into submodules which can be executed in parallel.

A. Joint Radio and Computational Resource Allocation

We aim to jointly optimize the users' transmit powers and the computational resources assigned to the users, in order to minimize the total uplink transmit power while maximizing the minimum SE throughout the network and providing uniform quality of service to all the users. This optimization problem can be formulated as:

$$\underset{\{p_k\}, \{f_k^{\text{CPU}}\}, \{f_{l,k}^{\text{AP}}\}, \nu}{\text{minimize}} \quad \sum_{k=1}^K p_k - \nu \quad (7a)$$

$$\text{s.t.} \quad \frac{b_k}{B \text{SE}_k} + \frac{w_k}{f_k^{\text{CPU}} + \sum_{l \in \mathcal{M}_k} f_{l,k}^{\text{AP}}} \leq \tilde{\mathcal{L}}_k, \forall k, \quad (7b)$$

$$\text{SE}_k \geq \nu, \forall k, \quad (7c)$$

$$\sum_{k=1}^K f_k^{\text{CPU}} \leq f^{\text{CPU}}, \quad (7d)$$

$$\sum_{k \in \mathcal{K}_l} f_{l,k}^{\text{AP}} \leq f_l^{\text{AP}}, \forall l, \quad (7e)$$

$$f_k^{\text{CPU}} \geq 0, \forall k, \quad (7f)$$

$$f_{l,k}^{\text{AP}} \geq 0, \forall k, \forall l, \quad (7g)$$

$$0 \leq p_k \leq p_{\max}, \forall k, \quad (7h)$$

where $\tilde{\mathcal{L}}_k = \mathcal{L}_k - (2b_k M\xi / C_{\text{FH}})$, p_{\max} is the maximum transmit power per user, and ν is a new variable representing the minimum instantaneous SE among the users that has to be maximized.

This problem is clearly non-convex with respect to $\{p_k\}$ due to the non-convexity (non-concavity) of the latency constraint (7b) and the minimum SE constraint (7c). Moreover, the coupling between the uplink transmit powers renders this problem difficult to solve. We resort here to *sequential convex programming*, that is an iterative optimization framework wherein in each iteration we optimize a related convex approximation of the original problem. Specifically, letting $\mathbf{p} = [p_1 \cdots p_K]^T$, notice that the uplink instantaneous SE for user k can be expressed as

$$\text{SE}_k = \frac{\tau_u}{\tau_c} \log_2 \left(1 + \frac{\text{num}_k(\mathbf{p})}{\text{den}_k(\mathbf{p})} \right) = \frac{\tau_u}{\tau_c} (\log_2(\text{num}_k(\mathbf{p}) + \text{den}_k(\mathbf{p})) - \log_2(\text{den}_k(\mathbf{p}))), \quad (8)$$

where $\text{num}_k(\mathbf{p})$ and $\text{den}_k(\mathbf{p})$ describe the numerator and the denominator of (4), respectively, which are functions of the power coefficients. As $\log_2(\cdot)$ is increasing and the summation preserves concavity, the SE expression in (8) is the difference of two concave functions. Recalling that any concave function is upper-bounded by its Taylor expansion around any given point $\mathbf{p}^{(0)}$, a concave lower-bound of SE_k is obtained as

$$\begin{aligned} \text{SE}_k(\mathbf{p}) &\geq \log_2(\text{num}_k(\mathbf{p}) + \text{den}_k(\mathbf{p})) - \log_2(\text{den}_k(\mathbf{p}^{(0)})) - \nabla_{\mathbf{p}}^T \log_2(\text{den}_k(\mathbf{p})) \Big|_{\mathbf{p}=\mathbf{p}^{(0)}} (\mathbf{p} - \mathbf{p}^{(0)}) \\ &= \widetilde{\text{SE}}_k(\mathbf{p}, \mathbf{p}^{(0)}). \end{aligned} \quad (9)$$

Hence, the latency constraint (7b) and the minimum SE constraint in (7c) are approximated and convexified by taking

$$\frac{b_k}{B \widetilde{\text{SE}}_k(\mathbf{p}, \mathbf{p}^{(0)})} + \frac{w_k}{f_k} \leq \widetilde{\mathcal{L}}_k, \quad \text{and} \quad \widetilde{\text{SE}}_k(\mathbf{p}, \mathbf{p}^{(0)}) \geq \nu, \quad \forall k,$$

for any feasible choice of $\mathbf{p}^{(0)}$. Note that, the arguments above hold if the elements of the receive combining vector do not depend on the uplink transmit powers. However, in general, the receive combining vector can include a further dependency on \mathbf{p} , for instance in the case of P-MMSE receive combining, as shown in (5). This issue can be simply tackled by treating the combining vectors at the n -th iteration of the SCA optimization framework as constant with respect to the current uplink transmit powers $\mathbf{p}^{(n)}$, and being exclusively function of $\mathbf{p}^{(n-1)}$. Finally, we introduce the vector of the computational resources $\mathbf{f} \in \mathbb{Z}^{K+KL}$ defined as

$$\mathbf{f} = [f_1^{\text{CPU}}, \dots, f_K^{\text{CPU}}, f_{1,1}^{\text{AP}}, f_{2,1}^{\text{AP}}, \dots, f_{L,1}^{\text{AP}}, f_{1,2}^{\text{AP}}, f_{2,2}^{\text{AP}}, \dots, f_{L,K}^{\text{AP}}]^{\text{T}},$$

such that we can write $f_k = \mathbf{b}_k^{\text{T}} \mathbf{f}$, $\forall k$, with $\mathbf{b}_k \in \{0, 1\}^{K+KL}$ being a fixed binary vector determined by the user-centric setup. Specifically, $\mathbf{b}_k = [\mathbf{e}_k^{\text{T}} \quad \hat{\mathbf{b}}_k^{\text{T}}]^{\text{T}}$, where \mathbf{e}_k is the k -th column of \mathbf{I}_K and $\hat{\mathbf{b}}_k \in \{0, 1\}^{KL}$ such that its element, $\hat{\mathbf{b}}_k((k-1)L+l)$ is either 1 if AP l serves user k with all its antennas or 0 otherwise. The vector $\hat{\mathbf{b}}_k$ can be easily constructed upon \mathbf{D}_{lk} as $\hat{\mathbf{b}}_k((k-1)L+l) = \text{tr}(\mathbf{D}_{lk})/M$, $\forall k, \forall l$. Similarly, we define $\mathbf{c}_l = [\mathbf{0}_K^{\text{T}} \quad \hat{\mathbf{c}}_l^{\text{T}}]^{\text{T}}$, and construct the vector $\hat{\mathbf{c}}_l \in \{0, 1\}^{KL}$ upon \mathbf{D}_{lk} as $\hat{\mathbf{c}}_l((k-1)L+l) = \text{tr}(\mathbf{D}_{lk})/M$, $\forall k, \forall l$. Hence, the optimization problem at the n -th iteration of the proposed SCA method can be formulated as

$$\underset{\mathbf{p}^{(n)}, \mathbf{f}^{(n)}, \nu}{\text{minimize}} \quad \mathbf{1}_K^{\text{T}} \mathbf{p}^{(n)} - \nu \tag{10a}$$

$$\text{s.t.} \quad \frac{b_k}{B \widetilde{\text{SE}}_k(\mathbf{p}^{(n)}, \mathbf{p}^{(n-1)})|_{\mathbf{v}_k^{(n)}(\mathbf{p}^{(n-1)})}} + \frac{w_k}{\mathbf{b}_k^{\text{T}} \mathbf{f}^{(n)}} \leq \widetilde{\mathcal{L}}_k, \quad \forall k, \tag{10b}$$

$$\widetilde{\text{SE}}_k(\mathbf{p}^{(n)}, \mathbf{p}^{(n-1)})|_{\mathbf{v}_k^{(n)}(\mathbf{p}^{(n-1)})} \geq \nu, \quad \forall k, \tag{10c}$$

$$\sum_{k=1}^K \mathbf{f}^{(n)}(k) \leq f^{\text{CPU}}, \tag{10d}$$

$$\mathbf{c}_l^{\text{T}} \mathbf{f}^{(n)} \leq f_l^{\text{AP}}, \quad \forall l, \tag{10e}$$

$$\mathbf{0}_K \preceq \mathbf{p}^{(n)} \preceq p_{\max} \cdot \mathbf{1}_K, \tag{10f}$$

$$\mathbf{f}^{(n)} \in \mathbb{R}_{>0}^{K+KL}. \tag{10g}$$

where the constraint (10g) is the continuous relaxation of the original constraint $\mathbf{f}^{(n)} \in \mathbb{Z}_{>0}^{K+KL}$ (the real-valued entries of the optimal \mathbf{f} are then rounded). For an arbitrary iteration n of the

SCA method, $\widetilde{\text{SE}}_k(\mathbf{p}^{(n)}, \mathbf{p}^{(n-1)})$ is a suitable convex approximation of $\text{SE}_k(\mathbf{p}^{(n)})$, as the following properties are fulfilled [34]:

$$\text{SE}_k(\mathbf{p}^{(n)}) \geq \widetilde{\text{SE}}_k(\mathbf{p}^{(n)}, \mathbf{p}^{(n-1)}), \quad \forall n, k, \quad (11a)$$

$$\text{SE}_k(\mathbf{p}^{(n-1)}) = \widetilde{\text{SE}}_k(\mathbf{p}^{(n-1)}, \mathbf{p}^{(n-1)}), \quad \forall n, k, \quad (11b)$$

$$\nabla_{\mathbf{p}} \text{SE}_k(\mathbf{p}^{(n-1)}) = \nabla_{\mathbf{p}} \widetilde{\text{SE}}_k(\mathbf{p}^{(n-1)}, \mathbf{p}^{(n-1)}), \quad \forall n, k, \quad (11c)$$

where $\mathbf{p}^{(n-1)}$ is the optimal solution to problem (10) at the iteration $n - 1$. According to the theory in [34], by virtue of the properties (11a), (11b), the sequence consisting of the objective functions (10a) evaluated at the optimal points is monotonically decreasing and converges to a finite limit. Moreover, this limit, due to the property (11c), is the value that the original objective function (7a) attains at a point satisfying the Karush-Kuhn-Tucher (KKT) conditions of problem (7). We provide here a brief proof that resembles the arguments in [30].

Proof: Let us denote the objective function of problem (7) and problem (10) as $\mathcal{F}(\mathbf{p}^{(n)}, \nu)$ and $\widetilde{\mathcal{F}}(\mathbf{p}^{(n)}, \nu)$, respectively. Let $\mathbf{p}^{(n)}$ be the solution at the n -th iteration. It holds that

$$\mathcal{F}(\mathbf{p}^{(n-1)}, \nu) = \widetilde{\mathcal{F}}(\mathbf{p}^{(n-1)}, \nu) \geq \widetilde{\mathcal{F}}(\mathbf{p}^{(n)}, \nu) = \mathcal{F}(\mathbf{p}^{(n)}, \nu). \quad (12)$$

The first equality is trivial; the inequality holds as $\mathbf{p}^{(n)}$ is the optimal solution of problem (10). Note that $\mathbf{p}^{(n)}$ satisfies the constraint (10b) and (10c), which are stricter than (7b) and (7c), respectively, because of the property (11a). Hence, $\mathbf{p}^{(n)}$ must necessarily satisfy the original constraint (7b) and (7c) too, and yields the same objective value for the original problem. This justifies the last equality in (12). Hence, $\mathcal{F}(\mathbf{p}^{(n)}, \nu)$ decreases iteratively as n increases, and converges to a finite limit since $\mathcal{F}(\mathbf{p}^{(n)}, \nu)$ is lower bounded and the feasible region is a compact set. It follows that an optimal point satisfies the KKT conditions of the original problem, since problem (7) and (10) have the same objective and derivative values at the optimal point. ■

Algorithm 1, to be run at the CPU, summarizes the proposed SCA method solving problem (7).

B. Feasibility

The following conditions are necessary but not sufficient for the problem in (7) to admit a non-empty feasible set satisfying all the constraints (7b)-(7h):

$$\begin{cases} R_k > b_k / \widetilde{\mathcal{L}}_k, \forall k, \\ \sum_{k=1}^K \frac{w_k}{\widetilde{\mathcal{L}}_k - b_k / R_k} < f^{\text{CPU}} + \sum_{l \in \mathcal{Z}} f_l^{\text{AP}}, \\ f^{\text{CPU}} \gg f_l^{\text{AP}}, \forall l \in \mathcal{Z}, \end{cases} \quad (13)$$

Algorithm 1 SCA algorithm for Problem (7)

Input: Any choice of feasible transmit powers $\mathbf{p}^{(0)}$;

- 1: Initialize $n \leftarrow 1$;
- 2: **repeat**
- 3: Let $\mathbf{p}^*, \mathbf{f}^*$ the optimal solutions of problem (10);
- 4: $\mathbf{p}^{(n)} \leftarrow \mathbf{p}^*$;
- 5: $\mathbf{f}^{(n)} \leftarrow \mathbf{f}^*$;
- 6: $n \leftarrow n + 1$;
- 7: **until** convergence

Output: \mathbf{p}, \mathbf{f} ;

where $\mathcal{Z} = \bigcup_{k=1}^K \mathcal{M}_k$. The set of conditions in (13) guarantees that each user is able to transmit with a rate supporting the effective maximum tolerable latency, while the second condition in (13) checks that the overall computational resources required by all the users might be afforded by the CPU and all the *active* APs in the network. These conditions are necessary but not sufficient, due to the distributed nature of the considered resource allocation.³ However, the feasibility of problem (7) is likely to be ensured if the remote cloud server (i.e., the CPU) is computationally much more powerful than any APs in the system (third condition in (13)), such that it has enough computing resources to possibly cope with the AP's temporary lack of available computing resources, and to meet user's demand in a centralized fashion. Besides, a non-empty feasible set for problem (7) can anyhow be enforced by a proper joint admission control and computation-offloading strategies [35], [36].

With respect to problem (10), it suffices that these conditions are satisfied at the first iteration, as in the following iterations the problem feasibility is enforced by the constraints. An effective heuristic choice for the initial set of the uplink transmit powers is given by the popular fractional power control algorithm. This scheme selects the uplink power of the k -th user as

$$p_k = p_{\max} \frac{(\sum_{l \in \mathcal{M}_k} \beta_{kl})^\vartheta}{\max_{i \in \mathcal{S}_k} (\sum_{l \in \mathcal{M}_i} \beta_{il})^\vartheta}, \quad (14)$$

where $\vartheta \in [-1, 1]$ is a design parameter controlling the power allocation behavior. In general, by increasing ϑ we favor the sum SE, as more power is used by the users with better channel conditions, while fairness is promoted by using lower values of ϑ . The above approach for

³If all the APs would share their own computational resources, thereby providing computational offloading in a centralized fashion, then the first two conditions in (13) would be sufficient to guarantee a non-empty feasible set for problem (7).

evaluating the feasibility of problem (7) a priori, presupposes a pre-determined power control allocation (e.g., the fractional power control strategy described in eq. (14)) to evaluate the per-user uplink rates $\{R_k\}$ that come into play in (13). However, the chosen initial set of the uplink powers might not be a feasible point for problem (7).

An alternative, and rigorous, feasibility check providing also a feasible set of uplink transmit powers is the two-stage procedure that is presented next. In the first stage, we seek for a set of the user computational rates $\{f_k = \mathbf{b}_k^T \mathbf{f}\}$ fulfilling the computational latency constraints, that is $\mathbf{b}_k^T \mathbf{f} \geq w_k / \tilde{\mathcal{L}}_k, \forall k$, and within the computational budget limits in eqs. (7d), (7e). This consists in solving the following linear program:

$$\underset{\mathbf{f} \in \mathbb{R}_{>0}^{K+KL}}{\text{minimize}} \quad \mathbf{1}_{K+KL}^T \mathbf{f} \quad \text{s.t.} \quad \mathbf{B} \mathbf{f} \succeq \mathbf{a}, \quad (15)$$

where

$$\mathbf{B} = \begin{bmatrix} \mathbf{b}_1^T & \dots & \mathbf{b}_K^T & -\mathbf{b}_{\text{CPU}}^T & -\mathbf{c}_1^T & \dots & -\mathbf{c}_L^T \end{bmatrix}^T \in \{-1, 0, 1\}^{(K+L+1) \times (K+KL)}, \quad (16)$$

$$\mathbf{a} = \begin{bmatrix} \frac{w_1}{\tilde{\mathcal{L}}_1} & \dots & \frac{w_K}{\tilde{\mathcal{L}}_K} & -f^{\text{CPU}} & -f_1^{\text{AP}} & \dots & -f_L^{\text{AP}} \end{bmatrix}^T \in \mathbb{R}^{K+L+1}, \quad (17)$$

$$\mathbf{b}_{\text{CPU}} = [\mathbf{1}_K^T \quad \mathbf{0}_{KL}^T]^T \in \{0, 1\}^{K+L+1}. \quad (18)$$

If problem (15) admits global optimal solution, then we move to the second stage, and seek for a set of users' computational rates $\{f_k = \mathbf{b}_k^T \mathbf{f}\}$ minimizing the maximum SE requirement:

$$\underset{\mathbf{f}}{\text{minimize}} \quad \max_k \frac{b_k/B}{\tilde{\mathcal{L}}_k - \frac{w_k}{\mathbf{b}_k^T \mathbf{f}}} \quad (19a)$$

$$\text{s.t.} \quad \sum_{k=1}^K \mathbf{f}(k) \leq f^{\text{CPU}}, \quad (19b)$$

$$\mathbf{c}_l^T \mathbf{f} \leq f_l^{\text{AP}}, \forall l, \quad (19c)$$

$$\mathbf{f} \in \mathbb{R}_{>0}^{K+KL}, \quad (19d)$$

which can be written in epigraph form as

$$\underset{\mathbf{f}}{\text{minimize}} \quad t \quad (20a)$$

$$\text{s.t.} \quad \mathbf{b}_k^T \mathbf{f} \leq \frac{w_k}{\tilde{\mathcal{L}}_k - \frac{b_k}{tB}}, \forall k, \quad (20b)$$

$$(19b)-(19d), \quad (20c)$$

and can be efficiently solved by using the *bisection method* [37], as detailed in Algorithm 2. Let \mathbf{f}^* denote the optimal solution of problem (19), obtained via Algorithm 2. According to (6), it must hold

$$\frac{b_k}{R_k(\mathbf{p})} + \frac{w_k}{\mathbf{b}_k^T \mathbf{f}^*} \leq \tilde{\mathcal{L}}_k, \quad \forall k \Leftrightarrow R_k(\mathbf{p}) \geq \frac{b_k}{\tilde{\mathcal{L}}_k - \frac{w_k}{\mathbf{b}_k^T \mathbf{f}^*}}, \quad \forall k, \quad (21)$$

Algorithm 2 Bisection method for Problem (20)

```

1: Initialize  $\varepsilon \leftarrow 0.005$ ;  $\epsilon \leftarrow 10^{-5}$ ;  $t_{\text{low}} \leftarrow \max_k \frac{b_k}{B\tilde{\mathcal{L}}_k}$ ;  $t_{\text{up}} \leftarrow \max_k \frac{b_k}{\varepsilon B\tilde{\mathcal{L}}_k}$ ;
2: while  $t_{\text{up}} - t_{\text{low}} > \epsilon$  do
3:    $t = (t_{\text{up}} + t_{\text{low}})/2$ 
4:   if the problem: find  $\mathbf{f}$  s.t. (20b)-(20c) is feasible then
5:      $t_{\text{up}} \leftarrow t$ ;
6:     Let  $\mathbf{f}^*$  be the optimal solution of the feasibility problem;
7:   else
8:      $t_{\text{low}} \leftarrow t$ ;
9:   end if
10: end while
Output:  $\mathbf{f}^*$ ;

```

which represents a *quality-of-service* (QoS) requirement. Let us translate the rightmost inequality in (21) to the following instantaneous SINR requirement

$$\frac{p_k g_{kk}}{\sum_{i \neq k}^K p_i (g_{ki} + c_{ki}) + p_k c_{kk} + \sigma^2 \|\mathbf{v}_k^H \mathbf{D}_k\|^2} \geq \frac{2^{z_k} - 1}{\tilde{\gamma}_k}, \quad \forall k, \quad (22)$$

where $g_{ki} = |\mathbf{v}_k^H \mathbf{D}_k \hat{\mathbf{h}}_i|^2$, $c_{ki} = \mathbf{v}_k^H \mathbf{D}_k \mathbf{C}_i \mathbf{D}_k \mathbf{v}_k$, and

$$z_k = \frac{b_k}{\frac{\tau_u}{\tau_c} B \left(\tilde{\mathcal{L}}_k - \frac{w_k}{\mathbf{b}_k^T \mathbf{f}^*} \right)}.$$

Hence, the instantaneous SINR requirement in (22) can be rewritten as the vector inequality

$$\mathbf{p} \succeq \Upsilon \mathbf{G}^{-1} (\mathbf{Z} \mathbf{p} + \sigma^2 \mathbf{u}), \quad (23)$$

where $\Upsilon = \text{diag}(\tilde{\gamma}_1, \dots, \tilde{\gamma}_K)$, $\mathbf{u} = \left[\|\mathbf{v}_1^H \mathbf{D}_1\|^2 \ \dots \ \|\mathbf{v}_K^H \mathbf{D}_K\|^2 \right]^T$, and

$$[\mathbf{G}]_{ki} = \begin{cases} g_{kk} - c_{kk} \tilde{\gamma}_k, & \text{if } k = i, \\ 0, & \text{otherwise,} \end{cases} \quad [\mathbf{Z}]_{ki} = \begin{cases} 0, & \text{if } k = i, \\ g_{ki} + c_{ki}, & \text{otherwise.} \end{cases} \quad (24)$$

Hence, a set of non-negative uplink transmit powers \mathbf{p} , that depends on the small-scale fading channel realizations, can be determined capitalizing on the requirement in (22). The set of SINR targets $\{\tilde{\gamma}_k\}$ is feasible, if and only if all the diagonal elements of \mathbf{G} are non-negative⁴, and the Perron-Frobenius eigenvalue of the matrix $\Upsilon \mathbf{G}^{-1} \mathbf{Z}$, denoted by ρ , is real and non-negative, and $\rho < 1$ [38]. If these conditions are satisfied, then $\mathbf{I}(\mathbf{p}) = \Upsilon \mathbf{G}^{-1} (\mathbf{Z} \mathbf{p} + \sigma^2 \mathbf{u})$ is

⁴Note that it is not guaranteed that $g_{kk} - c_{kk} \tilde{\gamma}_k \geq 0, \forall k$.

Algorithm 3 Standard power control algorithm assuming P-MMSE

Input: $\{\Upsilon\}$, $\{\mathbf{C}_k\}$, $\{\mathbf{D}_k\}$, $\{\hat{\mathbf{h}}_k\}$;

- 1: Initialize $n = 0$, $\chi = 1$; $\mathbf{p}^{(0)}$; $\mathbf{v}(\mathbf{p}^{(0)})$;
- 2: **while** $\chi > 0.005$ **do**
- 3: Compute $\mathbf{G}(\mathbf{p}^{(n)})$, $\mathbf{Z}(\mathbf{p}^{(n)})$ according to (24);
- 4: Compute $\rho(\Upsilon \mathbf{G}^{-1} \mathbf{Z})$;
- 5: **if** \mathbf{G} is non-negative **and** $\rho < 1$ **then**
- 6: $n \leftarrow n + 1$;
- 7: $\mathbf{p}^{(n)} \leftarrow \mathbf{I}(\mathbf{p}^{(n-1)})$;
- 8: Compute $\mathbf{v}_k(\mathbf{p}^{(n)})$ according to (5), $\forall k$;
- 9: $\chi \leftarrow \max_k \left| \frac{p_k^{(n)} - p_k^{(n-1)}}{p_k^{(n-1)}} \right|$;
- 10: **else**
- 11: **Output:** The SINR targets $\{\tilde{\gamma}_k\}$ are not feasible; **break**;
- 12: **end if**
- 13: **end while**

Output: $\mathbf{p}^* \leftarrow \mathbf{p}^{(n)}$;

a *standard interference function* [39], and an optimal solution for the uplink transmit powers, is obtained iteratively through the *standard power control algorithm* [39] as $\mathbf{p}^{(n)} = \mathbf{I}(\mathbf{p}^{(n-1)})$, for any given initial choice $\mathbf{p}^{(0)}$.⁵ Algorithm 3 specifies the steps of the *standard power control algorithm* based on sequential optimization, and assuming P-MMSE. If Algorithm 3 converges to an optimal solution, say \mathbf{p}^* , then this solution can be used as initial feasible choice, that is $\mathbf{p}^{(0)} = \mathbf{p}^*$ for Algorithm 1 that solves the optimization problem in (10). For the considered P-MMSE combining, also notice that whenever a set of feasible uplink transmit powers is found (i.e., line 7 of Algorithm 3), the receive combining vectors $\{\mathbf{v}_k\}$ must be updated accordingly, such that the matrix $\Upsilon \mathbf{G}^{-1} \mathbf{Z}$ at the next iteration is properly computed.

IV. CELL-FREE VERSUS CELLULAR MASSIVE MIMO IN MEC

In this section, we numerically evaluate the performance provided by the proposed joint radio and computational resource allocation for CF-mMIMO systems and compare it with the performance attained by a cellular massive MIMO deployment. To this end, we extend our proposed framework to a traditional multicell massive MIMO system.

⁵This optimal solution satisfies all the inequalities in (23) with equality, and minimizes the sum of the transmitted powers [39].

A. Cellular Massive MIMO System Model

With respect to the system model described in Section II, we can simply treat a cellular massive MIMO network as a special case of a CF-mMIMO network wherein each user is exclusively served by one of the APs. An uplink achievable SE for user k served by AP l , is given by

$$\overline{\text{SE}}_{lk}^{(\text{cell})} = \frac{\tau_u}{\tau_c} \mathbb{E} \left\{ \log_2(1 + \text{SINR}_{lk}^{(\text{cell})}) \right\}, \quad \text{bit/s/Hz} \quad (25)$$

where

$$\text{SINR}_{lk}^{(\text{cell})} = \frac{p_k |\mathbf{v}_{lk}^H \hat{\mathbf{h}}_{lk}|^2}{\sum_{i \neq k}^K p_i |\mathbf{v}_{lk}^H \hat{\mathbf{h}}_{li}|^2 + \mathbf{v}_{lk}^H \left(\sum_{i=1}^K p_i \mathbf{C}_{li} \right) \mathbf{v}_{lk} + \sigma^2 \|\mathbf{v}_{lk}\|^2}, \quad (26)$$

for an arbitrary receive combining vector $\mathbf{v}_{lk} \in \mathbb{C}^M$. The effective uplink SINR, $\text{SINR}_{lk}^{(\text{cell})}$, is maximized by using the *Local-MMSE*⁶ (L-MMSE) receive combining, which is given by

$$\mathbf{v}_{lk}^{\text{L-MMSE}} = p_k \left(\sum_{i=1}^K p_i (\hat{\mathbf{h}}_{li} \hat{\mathbf{h}}_{li}^H + \mathbf{C}_{li}) + \sigma^2 \mathbf{I}_M \right)^{-1} \hat{\mathbf{h}}_{lk}. \quad (27)$$

Notice that L-MMSE is not scalable but can be used as a benchmark, since it constitutes the optimal combining scheme for cellular networks [13].

B. Joint Radio and Computational Resource Allocation in Cellular Massive MIMO

For cellular networks, we can reasonably assume that only the serving AP offers computational facility to its user terminals. Hence, using the same notation as in (7), we can formulate the joint radio and computational resource allocation problem for cellular networks as

$$\underset{\{p_k\}, \{f_{l,k}^{\text{BS}}\}, \{t_l\}}{\text{minimize}} \quad \sum_{k=1}^K p_k - \sum_{l=1}^L t_l \quad (28a)$$

$$\text{s.t.} \quad \frac{b_k}{B \text{SE}_{lk}} + \frac{w_k}{f_{l,k}^{\text{BS}}} \leq \mathcal{L}_k^{\text{cell}}, \quad \forall k, l \in \mathcal{M}_k, \quad (28b)$$

$$\text{SE}_{lk} \geq t_l, \quad \forall k, l \in \mathcal{M}_k, \quad (28c)$$

$$\sum_{k \in \mathcal{K}_l} f_{l,k}^{\text{BS}} \leq f_l^{\text{BS}}, \quad \forall l, \quad (28d)$$

$$f_{l,k}^{\text{BS}} \geq 0, \quad \forall k, l \in \mathcal{M}_k, \quad (28e)$$

$$0 \leq p_k \leq p_{\max}, \quad \forall k, \quad (28f)$$

where SE_{lk} represents the instantaneous SE, that is the value attained by (25) without expectation. $\mathcal{L}_k^{\text{cell}}$ denotes the maximum tolerable latency for user k in the cellular setup. This latency value is presumably larger than its cell-free counterpart as it does not include the delay produced by the

⁶The AP in each cell performs MMSE combining on its own, only relying upon the local channel estimates.

fronthaul signalling (i.e., steps 2–5 in Fig. 1). Moreover, in (28), f_l^{BS} indicates the computational capability of AP l , expressed in CPU cycles per second. Here, BS stands for *base station*, and this notation is used to emphasize the fact that in a cellular network the APs are actually BS with more antennas and higher computational capability, $f_l^{\text{BS}} > f_l^{\text{AP}}$, than the APs of the cell-free setup. While $f_{l,k}^{\text{BS}}$ denotes the fraction of computational resources assigned to user k by its serving BS l . Lastly, t_l represents the minimum instantaneous SE among the users in cell l that has to be maximized. Hence, through the problem in (28), we aim to jointly optimize the users' transmit powers and the computational resources assigned to the users, by minimizing the total uplink transmit power while maximizing the minimum SE per cell, and providing uniform quality of service to all the users within the same cell. This per-cell max-min fairness power control for MEC results more effective than its network-wide variant, as in the latter case, the SE of all the users would be significantly penalized by the worst SE throughout the network. Problem (28) can be convexified via sequential optimization, using a similar methodology as for its cell-free counterpart proposed in this paper. Hence, for the cellular setup, the optimization problem at the n -th iteration of the SCA method can be formulated as

$$\underset{\mathbf{p}^{(n)}, \boldsymbol{\zeta}^{(n)}, \mathbf{t}}{\text{minimize}} \quad \mathbf{1}_K^T \mathbf{p}^{(n)} - \mathbf{1}_L^T \mathbf{t} \quad (29\text{a})$$

$$\text{s.t.} \quad \frac{b_k}{B \widetilde{\text{SE}}_{lk}(\mathbf{p}^{(n)}, \mathbf{p}^{(n-1)})|_{\mathbf{v}_{lk}^{(n)}(\mathbf{p}^{(n-1)})}} + \frac{w_k}{\boldsymbol{\zeta}^{(n)}(k)} \leq \mathcal{L}_k^{\text{cell}}, \quad \forall k, \forall l \in \mathcal{M}_k, \quad (29\text{b})$$

$$\widetilde{\text{SE}}_{lk}(\mathbf{p}^{(n)}, \mathbf{p}^{(n-1)})|_{\mathbf{v}_{lk}^{(n)}(\mathbf{p}^{(n-1)})} \geq \mathbf{t}(l), \quad \forall k, \forall l \in \mathcal{M}_k, \quad (29\text{c})$$

$$\tilde{\mathbf{c}}_l^T \boldsymbol{\zeta}^{(n)} \leq f_l^{\text{BS}}, \quad \forall l, \quad (29\text{d})$$

$$\mathbf{0}_K \preceq \mathbf{p}^{(n)} \preceq p_{\max} \cdot \mathbf{1}_K, \quad (29\text{e})$$

$$\boldsymbol{\zeta}^{(n)} \in \mathbb{R}_{>0}^K, \quad (29\text{f})$$

where $\mathbf{t} = [t_1, \dots, t_L]^T$, and $\widetilde{\text{SE}}_{lk}(\mathbf{p}^{(n)}, \mathbf{p}^{(n-1)})$ is a concave lower-bound of $\text{SE}_{lk}(\mathbf{p}^{(n)})$ around the point $\mathbf{p}^{(n-1)}$, obtained by using the same methodology as in (9). $\boldsymbol{\zeta}$ denotes a $K \times 1$ vector of optimization variables, where its k -th element, $\boldsymbol{\zeta}(k)$, represents the amount of computational resources allocated to user k . Note that, in the cellular setup, it holds that $\boldsymbol{\zeta}(k) = f_{l,k}^{\text{BS}}$, $l \in \mathcal{M}_k$. $\tilde{\mathbf{c}}_l \in \{0, 1\}^K$ is an auxiliary binary vector, where the k -th element is 1 if BS l serves user k , and 0 otherwise. The SCA algorithm solving problem (28) follows Algorithm 1, but in each iteration it computes the optimal solutions of (29). This algorithm is run in a centralized fashion by a network entity (e.g., one of the BSs).

Convergence and optimality of the SCA optimization are guaranteed, as $\widetilde{\text{SE}}_{lk}(\mathbf{p}^{(n)}, \mathbf{p}^{(n-1)})$

is a suitable convex approximation of $\text{SE}_{lk}(\mathbf{p}^{(n)})$. Regarding feasibility, problem (29) admits a non-empty feasible set if

$$\begin{cases} R_k > b_k/\tilde{\mathcal{L}}_k, \forall k \\ \sum_{k \in \mathcal{K}_l} \frac{w_k}{\mathcal{L}_k^{\text{cell}} - b_k/R_{lk}} < f_l^{\text{BS}}, \forall l \end{cases} \quad (30)$$

where $R_{lk} = B \times \text{SE}_{lk}$, is the uplink instantaneous rate of user k served by BS l . The conditions in (30) are necessary and sufficient to ensure the feasibility of the optimization problem (7). If jointly satisfied, then all the users are able to transmit their program with a rate supporting their effective maximum tolerable latency, while each BS has enough computing resources to meet user's demand for computational offloading.

C. Simulation Setup

We consider a coverage area of 1 km \times 1 km served by a total number of antennas $N = LM = 400$. For the cellular massive MIMO setup, we choose $L = 4$ BSs, equipped with $M = 100$ antennas each, and deployed as a regular grid with intersite distance (i.e., the distance between BSs in the vertical/horizontal direction) equal to 500 m. For the cell-free massive MIMO setup, we select $L = 100$ APs, equipped with $M = 4$ antennas each, and deployed as a regular grid with intersite distance equal to 100 m. For both the setups a wrap-around simulation technique is used to remove the edge effects of the (nominal) coverage area.

Both the massive MIMO systems operate at 2 GHz carrier frequency, over a communication bandwidth $B = 20$ MHz. The receiver noise power is conventionally set to -94 dBm, while the maximum transmit power per user is $p_{\text{max}} = 100$ mW. The TDD coherence block is $\tau_c = 200$ samples long, resulting from a coherence bandwidth of 100 kHz and a coherence time of 2 ms. As we focus only on the uplink performance, we assume that the TDD coherence block exclusively accommodates the uplink data transmission phase, hence $\tau_d = 0$, besides $\tau_p = K/2$ samples dedicated to the uplink training.

Both the setups serve the same set of $K = 20$ users, that are uniformly distributed at random over the coverage area. A random realization of users' locations defines a network snapshot, and determines a set of large-scale fading coefficients. These are computed according to the 3GPP Urban Microcell model defined in [40, Table B.1.2.1-1] as

$$\beta_{lk} \text{ [dB]} = -30.5 - 36.7 \log_{10} \left(\frac{d_{lk}}{1 \text{ m}} \right) + \text{SF}_{lk},$$

where d_{lk} is the 3D distance between AP (BS) l and user k , and whose minimum value is set to 10 m corresponding to the height difference between the APs (BSs) and the users. The coefficient $SF_{lk} \sim \mathcal{N}(0, \sigma_{\text{sh}}^2)$, which denotes a log-normal shadow fading with standard deviation $\sigma_{\text{sh}} = 4$, and spatial correlations from an (a) AP (BS) to different users, is modeled as

$$\mathbb{E} \{SF_{lk} SF_{ji}\} = \begin{cases} \sigma_{\text{sh}}^2 2^{-\delta_{ki}/9 \text{ m}}, & l = j, \\ 0, & l \neq j, \end{cases}$$

where δ_{ki} is the distance between user k and user i , and 9 meters is the decorrelation distance.

The spatial channel correlations, hence the channel correlation matrices $\{\mathbf{R}_{lk}\}$, are generated by using the popular *local scattering* model assuming jointly Gaussian angular distributions of the multipath components around the nominal azimuth and elevation angles, denoted by ϕ and θ , respectively. The random variations in the azimuth and elevation angles are assumed to be independent, and the corresponding angular standard deviations (ASDs) are $\sigma_\phi = \sigma_\theta = 15^\circ$, which represents strong spatial channel correlation. For small ASDs, that is $\sigma_\phi \leq 15^\circ$ and $\sigma_\theta \leq 15^\circ$, we can compute an approximate closed-form expression for the spatial correlation matrices $\{\mathbf{R}_{lk}\}$. An approximate spatial correlation matrix in closed form, valid for small ASDs, was provided in [15] for ULAs and two-dimensional space model. Similarly, [41] generalizes this result to uniform planar array in a three-dimensional world. In this study, we consider ULAs in a 3D space model. It is easy to show, following [41, Appendix C], that the (n, \bar{n}) th element of an arbitrary spatial channel correlation matrix⁷ can be approximately expressed as

$$[\mathbf{R}]_{n\bar{n}} \approx \frac{A_{n\bar{n}} \tilde{\sigma}_{n\bar{n}}}{\sigma_\phi} \exp \left\{ \frac{D_{n\bar{n}}^2 \sigma_\theta^2 (C_{n\bar{n}}^2 \sigma_\theta^2 \tilde{\sigma}_{n\bar{n}}^2 - 1)}{2} \right\} \exp \left\{ -j B_{n\bar{n}} C_{n\bar{n}} D_{n\bar{n}} \sigma_\theta^2 \tilde{\sigma}_{n\bar{n}}^2 \right\} \exp \left\{ -\frac{B_{n\bar{n}}^2 \tilde{\sigma}_{n\bar{n}}^2}{2} \right\}$$

where

$$\begin{aligned} A_{n\bar{n}} &= \beta \exp\{j2\pi d_{n\bar{n}}^{(h)} \sin(\phi) \cos(\theta)\}, & B_{n\bar{n}} &= 2\pi d_{n\bar{n}}^{(h)} \cos(\phi) \cos(\theta), \\ C_{n\bar{n}} &= -2\pi d_{n\bar{n}}^{(h)} \cos(\phi) \sin(\theta), & D_{n\bar{n}} &= -2\pi d_{n\bar{n}}^{(h)} \sin(\phi) \sin(\theta), \\ \tilde{\sigma}_{n\bar{n}} &= \frac{\sigma_\phi^2}{1 + C_{n\bar{n}}^2 \sigma_\phi^2 \sigma_\theta^2}, \end{aligned}$$

and $d_{n\bar{n}}^{(h)}$ being the horizontal antenna spacing between the n th and the \bar{n} th array elements in wavelengths. In our simulations, we set this spacing equal to 0.5 (half-wavelength distance).

As $\tau_p < K$, pilots are to be re-assigned across users. To this end, we resort to the joint pilot assignment and AP (BS)-user association described in [13, Section 5.4], so as to ensure that users

⁷The AP and user indices are omitted for the sake of brevity.

served by the same set of APs (same BS, for the cellular setup) are given orthogonal pilots. Concerning, instead, the power control, we will consider the same initial conditions for both the two considered setups. We assume that the initial choice for the feasible transmit powers of the SCA joint radio and computational resource allocation problem is $\mathbf{p}^{(0)} = p_{\max} \cdot \mathbf{1}_K$.

With regard to the computation-offloading and latency model, for the cell-free setup, we assume $f^{\text{CPU}} = 10^{11}$ cycles/s, while f_l^{AP} are uniformly distributed random integers from the interval $[10^9, 10^{10}]$ cycles/s. The latency requirements are equal for all the users in the network and $\mathcal{L}_k = 0.5$ s. The fronthaul capacity is $C_{\text{FH}} = 10$ Gbps, and the number of bits for quantization is set as $\xi = 16$. Concerning the cellular setup, we select $f_l^{\text{BS}} = \left\lceil (\sum_{l=1}^{L^{\text{AP}}} f_l^{\text{AP}} + f^{\text{CPU}}) / L^{\text{BS}} \right\rceil$, where L^{AP} is the number of APs in the cell-free setup, while L^{BS} is the number of BSs in the cellular setup, that is 100 and 4, respectively. This ensures the same number of available computational resources in the coverage area between the two considered setups. Lastly, the latency requirements for the cellular users is $\mathcal{L}_k^{\text{cell}} = 0.7$ s. Common to both setups, the number of bits needed to transfer the users' computational tasks, $\{b_k\}$, are uniformly distributed random integers from the interval $[1, 10]$ Mbits, and the number of CPU cycles needed to run the task itself is conventionally set as a linear function of b_k , that is $w_k = \alpha b_k$, with $\alpha = 50$ cycles/bit [29].

D. Performance Comparison

We are now ready to discuss the numerical results obtained from our simulations. Firstly, we focus on the radiated power consumption. In Fig. 2(a), we show the cumulative distribution function (CDF), obtained over 200 network snapshots, of the total uplink transmit power, expressed in Watt. This is computed as $\sum_{k=1}^K p_k$, with the uplink powers $\{p_k\}$ being the optimal solutions of the SCA problem (10) and (29) for cell-free and cellular massive MIMO, respectively. Numerical results reveal a dramatic transmit power saving for the CF-mMIMO users as compared to the cellular massive MIMO users. In particular, our power allocation strategy for MEC offloading enables a total uplink transmit power saving of 30%–40% with respect to its centralized counterpart in cellular massive MIMO, and 70%–80% with respect to an uplink full power transmission strategy, whose total transmit power consumption amounts 2 W. More specific considerations can be made for the transmit power of the single user. Fig. 2(b) shows the CDF of the uplink transmit power per user, expressed in mW, resulting from the proposed joint power and computational resource allocation. At high percentiles (i.e., the upper half of the CDF plot), where the transmit power consumption is more significant, we observe that the CF-

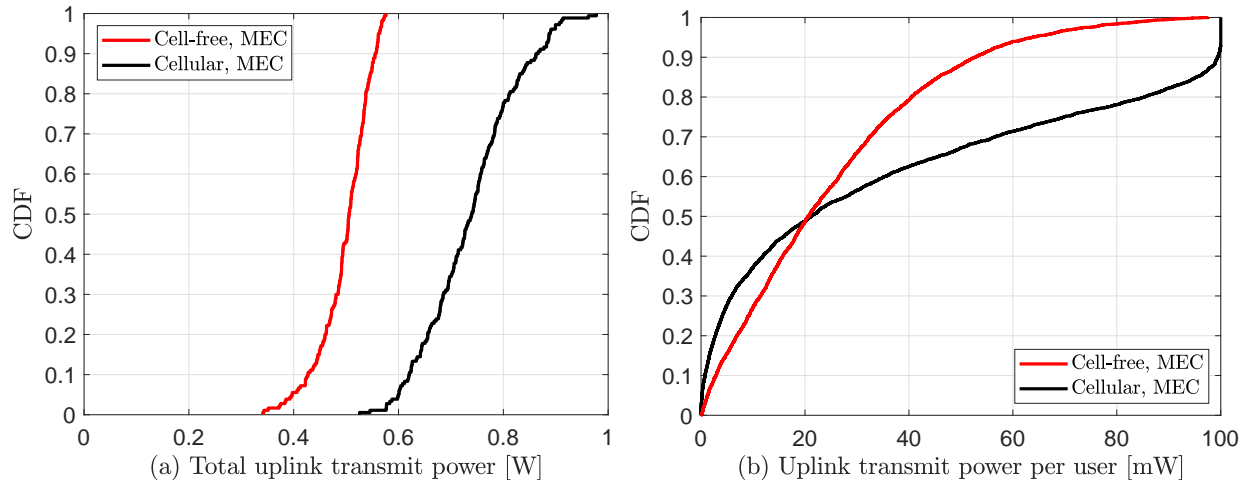


Fig. 2. CDF of the total (a) and per-user (b) uplink transmit power set by the proposed MEC strategy, for cell-free and cellular massive MIMO. The CDFs are obtained over 200 network snapshots. $K = 20$, and $p_{\max} = 100$ mW for all the users.

mMIMO users can considerably reduce their transmit power as compared to the cellular massive MIMO users. Interestingly, about 10% of the cellular users, presumably those at the cell-edge, need to transmit their computational task with full power, whereas the unlucky 10% of the cell-free users is likely to employ 50–80 mW. The transmit power saving at high percentiles can amazingly reach 50%. On the other hand, the lucky cellular users located at the cell center can leverage the massive BS array gain to substantially reduce their transmit power. This motivates the opposite trend at low percentiles, where the transmit power of the cell-free users is slightly higher. Nevertheless, this negative gap is negligible compared to the performance improvement at high percentiles, as demonstrated by Fig. 2(a) too.

Secondly, we focus on the allocation of the computational resources among the users. In Fig. 3(a), we show the CDF of the computational resources allocated to the single user by the proposed MEC offloading strategy, expressed in GHz ($10^9 \times$ cycles/s). While, Fig. 3(b) shows the CDF of the total allocated computational resources. These are computed as $\sum_{k=1}^K f_{l,k}^{\text{BS}}$ and $\sum_{k=1}^K (f_k^{\text{CPU}} + \sum_{l \in \mathcal{M}_k} f_{l,k}^{\text{AP}})$ for cellular and CF-mMIMO, respectively, and with the computational rates being the optimal solutions of the SCA problem (29) and (10), respectively. User's computational task size being equal, a smaller amount of remote CPU cycles/s is allocated to the cell-free users as compared to that of the cellular users, while fulfilling the latency requirements. This saving in terms of remote computational resources per user is particularly significant at low percentiles, reaching almost 40%, while is more uniform in terms of total allocated computational resources, ranging from 9% to 15%. To justify this double gain (i.e.,

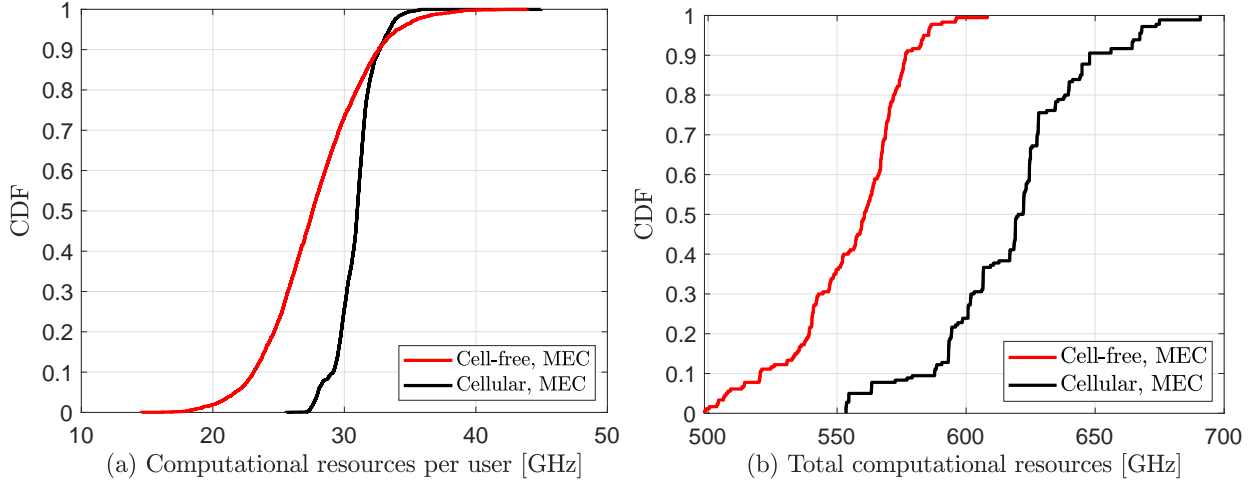


Fig. 3. CDF of the per-user (a) and total (b) computational resources allocated by the proposed MEC strategy, for cell-free and cellular massive MIMO. $f^{\text{CPU}} = 10^{11}$ Hz, $f_i^{\text{AP}} \sim \mathcal{U}(10^9, 10^{10})$ Hz, $f_l^{\text{BS}} = \lceil (\sum_{i=1}^{L^{\text{AP}}} f_i^{\text{AP}} + f^{\text{CPU}}) / L^{\text{BS}} \rceil$, $\mathcal{L}_k = 500$ ms and $\mathcal{L}_k^{\text{cell}} = 700$ ms, $\forall k$.

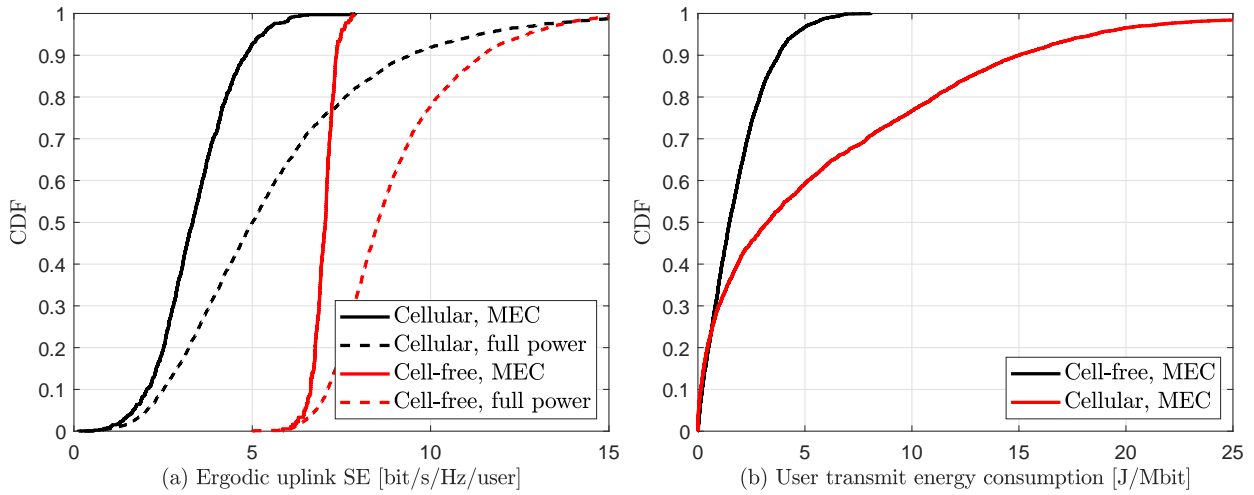


Fig. 4. (a) Ergodic uplink SE per user for cell-free and cellular massive MIMO, either with the proposed MEC offloading strategy or assuming full power transmissions. (b) Transmit energy consumption for cell-free and cellular users.

transmit power and allocated computational resources saving) of the cell-free setup over the cellular setup, we need to focus on the crucial role the SE plays. In Fig. 4, we show the ergodic uplink SE per user for cell-free and cellular massive MIMO, computed according to (3) and (25), respectively. Dashed curves, shown for benchmarking purposes, refer to the case that the users transmit at maximum power. Solid curves, instead, represent the SEs obtained by adopting the power allocation resulting from the proposed MEC offloading strategy. At first glance, we observe a degradation of the SE with a steeper CDF curve when MEC offloading is performed. This behaviour is a direct consequence of the optimization problem formulation (10) and (29). Indeed,

recall that the objective of the proposed joint power and computational resource allocation is to minimize the total uplink transmit power while maximizing the minimum instantaneous per-user SE. Reducing the transmit uplink powers generally leads to a SE degradation when using a MMSE-based combining scheme, while such a max-min fairness approach tends to flatten the CDF of the ergodic SE, as it produces uniform instantaneous SE values among the users. Our choice is motivated by the fact that, when sending the bits of the computational tasks for remote offloading, user's priority is saving as much transmit power as possible to prolong its battery lifetime, while still capitalizing on a fairly good SE to reduce its transmission latency, and more easily fulfill its latency requirements. Hence, our joint power and computational resource allocation provides an optimal balance between uplink transmit power consumption and uplink SE. Importantly, focusing only on the proposed MEC offloading strategy in Fig. 4(a), the uplink SE of the single cell-free user is, thanks to the macro-diversity gain, remarkably larger than that of the single cellular user, for instance, $2\times$ and $4\times$ in terms of median and 95%-likely SE, respectively. This significant SE gain reflects on the allocation of the computational resources and justifies the numerical results in Fig. 3. Indeed, a larger SE entails a shorter transmission latency (first term of (7b)), and gives the opportunity to allocate less computational resources since a longer computational latency (second term of (7b)) can be afforded in compliance with the latency constraint. The excellent balance between uplink transmit power consumption and uplink SE provided by our proposed approach is clearly shown in Fig. 4(b) which plots the CDF of the (normalized) transmit energy consumption, expressed in J/Mbit, for cell-free and cellular users. For an arbitrary user k , this is obtained as $E_k = p_k / (B \times SE_k)$ (or SE_{lk} for the cellular setup), with p_k being the optimal solution of the SCA problem (10) and (29) for cell-free and cellular massive MIMO, respectively, and SE_k being computed accordingly. As Fig. 4(b) shows, cell-free users can save a dramatic amount of transmit energy with respect to the cellular users, limiting their energy consumption to 5 J/Mbit.

V. MEC IN CELL-FREE MASSIVE MIMO: A CLOSER OUTLOOK

In this section, we explore more in detail the effectiveness of the proposed joint optimization of uplink power and computational resources for MEC-enabled CF-mMIMO, evaluating the interplay between uplink power, SE, allocated remote computational resources, and effective MEC offloading latency. Importantly, we also evaluate the soundness of the two problem feasibility checks described in Section III-B. In Fig. 5, we present the simulation results of one network

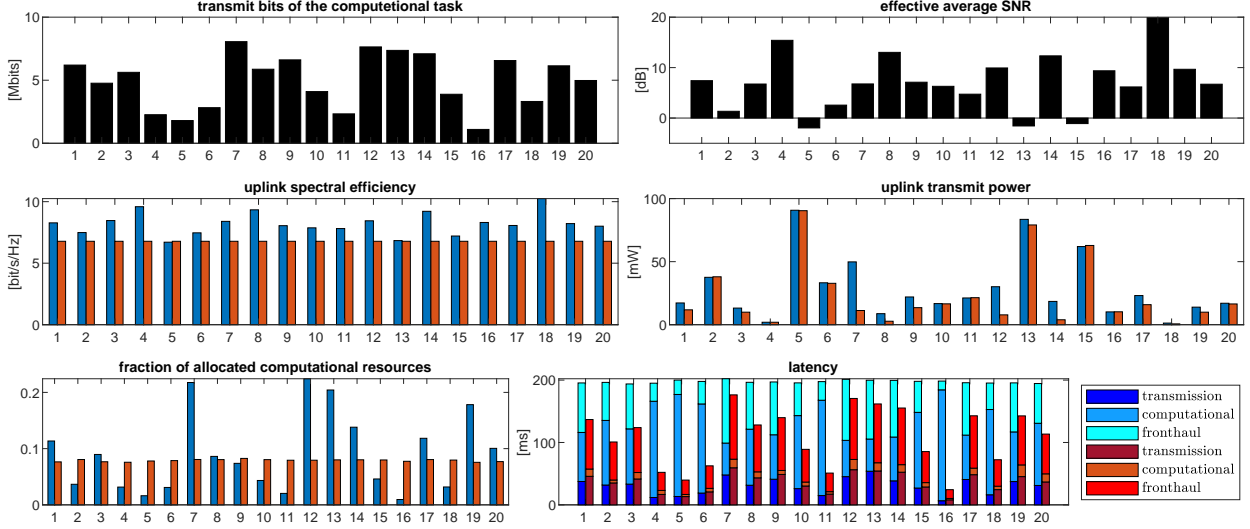


Fig. 5. Simulation results for one network snapshot, averaged over 200 channel realizations. x -axes report the user index. Reddish bars refer to the cell-free setup described in Section IV-C. Blueish bars refer to a cell-free setup with $\mathcal{L}_k = 200$ ms $\forall k$, $f^{\text{CPU}} = 10^{10}$ Hz, and $f_l^{\text{AP}} \sim \mathcal{U}(10^8, 10^9)$ Hz. Black bars (top sub-figures) refer to both the setups.

snapshot, where the final values are averaged over 200 channel realizations. For all the users, whose indices appear on the x -axes, we report: computational task size b_k in Mbits; effective average SNR computed as $\sum_{l \in \mathcal{M}_k} \beta_{lk} / \sigma^2$ and converted to dB; uplink SE in bit/s/Hz; uplink transmit power in mW; the fraction of allocated remote computational resources computed as $f_k / \left(\sum_{l \in \mathcal{M}_k} f_l^{\text{AP}} + f^{\text{CPU}} \right)$; and the effective MEC offloading latency consisting of transmission, computational and fronthaul latency. We consider two simulation setups: reddish bars refer to the cell-free setup described in Section IV-C, which we call “loose” setup for brevity; blueish bars refer to a “strict” cell-free setup with lower latency requirements, that is $\mathcal{L}_k = 200$ ms for all the users, and lower remote computational capability, that is $f^{\text{CPU}} = 10^{10}$ Hz, and $f_l^{\text{AP}} \sim \mathcal{U}(10^8, 10^9)$ Hz. The latter is of particular interest because highlights how the proposed joint optimization strategy operates under stricter constraints and modest computational resources. The two sub-figures on top (black bars) are in common to both the setups, as we fixed the simulation seed in order to obtain the same initial conditions. By inspecting Fig. 5, we observe that users with poor channel conditions, e.g., those with index 5, 13 and 15, naturally need to spend much more power than others to achieve the max-min fairness SE threshold. In the “strict” setup (blueish bars) the computational latency is generally dominant over the transmission latency. Indeed, unlike the computational latency that is subject to stricter constraints, the transmission latency can be further decreased by increasing the SE of the single users. This motivates the

non-uniform SE values despite the max-min fairness strategy. Increasing the SE represents a sort of last resort to comply with the strict latency requirements. While, notice that right the SE of the users with index 5, 13 and 15 are the lowest, and an attempt of increasing this performance would presumably violate the power budget constraint. Furthermore, in this regime of modest remote computational capability, users with demanding computational tasks are clearly assigned more remote computational resources (i.e., higher remote computational rates) than the rest of the users. For instance, the users with index 7, 12 and 13 are individually assigned about 20% of the total resources they have access to (which depends on their user-centric cluster). Lastly, the fronthaul latency is however proportional to the user’s task size, and is a constant in the optimization problem. In the “strict” setup, the effective MEC offloading time almost equals the latency requirement of 200 ms.

For the “loose” setup (reddish bars) we obtained different but equally interesting results. Firstly, we observe that the optimal uplink power is distributed similarly to the “strict” setup case, and reflects the effective average SNR, but with the total optimal uplink power being lower on average. Indeed, in such a regime with high remote computational capability, the computational latency can be arbitrarily reduced, and there is no need to excessively increase the uplink powers for moving the minimum SE threshold upward, and, in turn, reducing the transmission latency. This motivates the uniform SE values, which precisely reflect the max-min fairness policy. Interestingly, we observe that the effective MEC offloading time is far below the latency requirement of 500 ms. This result can be traced back to an implementation choice of the convex solver used in our simulations, that is MOSEK [42]. Indeed, the optimal computational rates lead to a uniform fractional allocation and, importantly, a (nearly) full utilization of the computational resources. That is, in absence of any constraints (for instance on the remote computational energy consumption), almost all the available computational resources are allocated, and the user’s computational latency considerably reduced. As an alternative, the amount of allocated remote computational resources may be reduced, conceding a longer computational latency yet fulfilling the “loose” latency requirement.

Finally, we focus on the two problem feasibility check approaches described in Section III-B. The approach based on evaluating the necessary conditions (13) conditioned on a prior uplink power control allocation is, for brevity, dubbed “rough” feasibility check. We dub instead “accurate” feasibility check, the approach consisting in solving the optimization problems (15), (19), and running Algorithm (3) to compute the starting point of the SCA procedure solving prob-

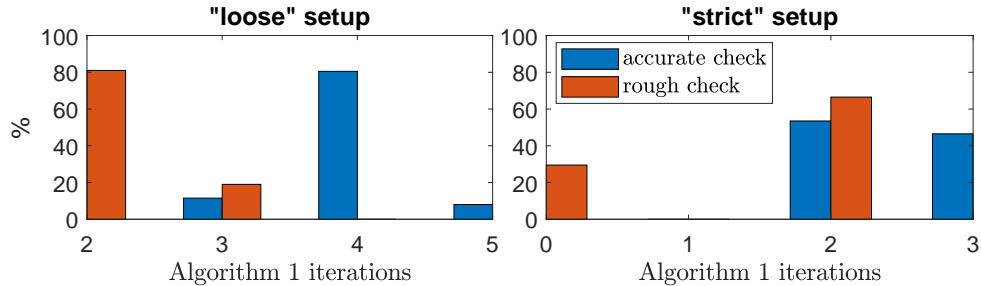


Fig. 6. Number of iterations needed for Algorithm 1 to converge, in case of initial uplink powers $\mathbf{p}^{(0)}$ selected by the proposed “rough” (reddish bars) and “accurate” (blueish bars) feasibility check approaches. Zero iterations indicates that the optimization problem is considered unfeasible. Results obtained for one network snapshot, averaged over 200 channel realizations, assuming the “loose” (left) and the “strict” (right) setup.

lem (10). Fig. 6 shows the number of iterations needed for Algorithm 1 to converge, in case of initial uplink powers $\mathbf{p}^{(0)}$ selected by the “rough” (reddish bars) and “accurate” (blueish bars) feasibility check approaches. These results are obtained for one network snapshot, averaged over 200 channel realizations, assuming the “loose” (left figure) and the “strict” (right figure) simulation setup. Regarding the “rough” feasibility check approach, we assume that the prior uplink power coefficients are set according to (14), with $\vartheta = -0.5$, which guarantees high level of fairness, in line with the max-min optimization strategy implicit in problem (7). Focusing on the left figure first, we observe that problem (10) is always feasible for both the approaches, thanks to the loose latency requirements, and the high remote computational capability. With the “rough” approach, Algorithm 1 converges in just two iterations 80% of the time, and in three iterations 20% of the time. This fast convergence is ensured by the fact that the fractional power control with exponent value -0.5 represents a sub-optimal choice for the max-min fairness policy, hence already close to the optimal solution of problem (7). With the “accurate” approach, Algorithm 1 converges in four iterations 80% of the time, and might even need five iterations. This slower convergence is due to the fact that the optimal feasible uplink powers resulting from Algorithm 3 are conceived to satisfy all the inequalities in (23) with equality, minimizing the total transmit power, and thereby are likely further from the optimal solution of problem (7). Concerning the “strict” setup, we interestingly observe that the “rough” feasibility check assesses problem (7) unfeasible 55% of the times, because the necessary conditions (13), initially subsuming a fractional power allocation with exponent -0.5, are not met. However, problem (7) admits a non-empty feasible set as proved by the “accurate” feasibility check, and in this setup fewer iterations are needed for Algorithm 1 to converge, as

the search space is presumably narrower. Summing up, the “rough” approach is helpful to speed up the problem feasibility check process, even though the fulfillment of conditions (13) does not guarantee that problem (7) is feasible (although very likely), and, importantly, if conditions (13) are not met, it does not necessarily mean that problem (7) is unfeasible. Conversely, the “accurate” approach provides a rigorous assessment on the problem feasibility, but requires solving two additional (albeit simple) optimization problems and running an iterative standard power control algorithm. A convenient rule-of-thumb may be evaluating the feasibility of problem (7) by firstly checking the necessary conditions (13), and in case of verdict “problem unfeasible” performing an “accurate” feasibility check.

VI. CONCLUSION

The problem of joint allocation of uplink powers and network computational resources in a MEC-enabled CF-mMIMO system was considered in this paper, with the aim of minimizing the total uplink power consumption under power budget and latency constraints, and simultaneously maximizing the minimum SE throughout the network. For efficiently solving such a challenging non-convex problem, an SCA algorithm and two approaches to priory assess the optimization problem feasibility were proposed. A detailed performance comparison between the proposed MEC-enabled CF-mMIMO architecture and its cellular counterpart was also provided, showing that CF-mMIMO is more suitable to support MEC applications than cellular massive MIMO. Numerical results also revealed the effectiveness of the proposed resource allocation strategy, which enables a significant reduction of users’ transmit power and energy consumption, transmission latency thanks to higher achievable SEs, and allocated remote computational resources.

REFERENCES

- [1] G. Interdonato and S. Buzzi, “The promising marriage of mobile edge computing and cell-free massive MIMO,” in *IEEE Int. Conf. on Commun. (ICC)*, 2022, submitted.
- [2] K. Yang, S. Ou, and H.-H. Chen, “On effective offloading services for resource-constrained mobile devices running heavier mobile internet applications,” *IEEE Commun. Mag.*, vol. 46, no. 1, pp. 56–63, Jan. 2008.
- [3] L. Y. Kumar K., Liu J. and B. B., “A survey of computation offloading for mobile systems,” *Mobile Netw. Appl.*, vol. 18, no. 1, p. 129–140, Apr. 2013.
- [4] S. Sardellitti, G. Scutari, and S. Barbarossa, “Joint optimization of radio and computational resources for multicell mobile-edge computing,” *IEEE Trans. Signal Inf. Process. Netw.*, vol. 1, no. 2, pp. 89–103, Jun. 2015.
- [5] P. Mach and Z. Becvar, “Mobile edge computing: A survey on architecture and computation offloading,” *IEEE Commun. Surveys Tuts.*, vol. 19, no. 3, pp. 1628–1656, 3rd Quart. 2017.

- [6] Y. Mao, C. You, J. Zhang, K. Huang, and K. B. Letaief, "A survey on mobile edge computing: The communication perspective," *IEEE Commun. Surveys Tuts.*, vol. 19, no. 4, pp. 2322–2358, 4th Quart. 2017.
- [7] "C-RAN white paper: The road towards green RAN," China Mobile Research Institute, 2014. [Online]. Available: <http://labs.chinamobile.com/cran>
- [8] A. Checko, H. L. Christiansen, Y. Yan, L. Scolari, G. Kardaras, M. S. Berger, and L. Dittmann, "Cloud RAN for mobile networks—A technology overview," *IEEE Communications Surveys Tutorials*, vol. 17, no. 1, pp. 405–426, 1st Quart. 2015.
- [9] J. Yuan, S. Jin, W. Xu, W. Tan, M. Matthaiou, and K. Wong, "User-centric networking for dense C-RANs: High-SNR capacity analysis and antenna selection," *IEEE Trans. Commun.*, vol. 65, no. 11, pp. 5067–5080, Nov. 2017.
- [10] C. Pan, M. El-kashlan, J. Wang, J. Yuan, and L. Hanzo, "User-centric C-RAN architecture for ultra-dense 5G networks: Challenges and methodologies," *IEEE Commun. Mag.*, vol. 56, no. 6, pp. 14–20, Jun. 2018.
- [11] H. Q. Ngo, A. Ashikhmin, H. Yang, E. G. Larsson, and T. L. Marzetta, "Cell-free massive MIMO versus small cells," *IEEE Trans. Wireless Commun.*, vol. 16, no. 3, pp. 1834–1850, Mar. 2017.
- [12] G. Interdonato, E. Björnson, H. Q. Ngo, P. Frenger, and E. G. Larsson, "Ubiquitous cell-free massive MIMO communications," *EURASIP J. Wireless Commun. and Netw.*, vol. 2019, no. 1, p. 197, 2019.
- [13] Özlem Tugfe Demir, E. Björnson, and L. Sanguinetti, "Foundations of user-centric cell-free massive MIMO," *Foundations and Trends® in Signal Processing*, vol. 14, no. 3-4, pp. 162–472, 2021.
- [14] T. L. Marzetta, E. G. Larsson, H. Yang, and H. Q. Ngo, *Fundamentals of Massive MIMO*. Cambridge University Press, 2016.
- [15] E. Björnson, J. Hoydis, and L. Sanguinetti, "Massive MIMO networks: Spectral, energy, and hardware efficiency," *Foundations and Trends® in Signal Processing*, vol. 11, no. 3-4, pp. 154–655, 2017.
- [16] S. Buzzi, C. D'Andrea, A. Zappone, and C. D'Elia, "User-centric 5G cellular networks: Resource allocation and comparison with the cell-free massive MIMO approach," *IEEE Trans. Wireless Commun.*, vol. 19, no. 2, pp. 1250–1264, Feb. 2020.
- [17] G. Interdonato, P. Frenger, and E. G. Larsson, "Scalability aspects of cell-free massive MIMO," in *Proc. IEEE Int. Conf. on Commun. (ICC)*, May 2019, pp. 1–6.
- [18] E. Björnson and L. Sanguinetti, "Scalable cell-free massive MIMO systems," *IEEE Trans. Commun.*, vol. 68, no. 7, pp. 4247–4261, Jul. 2020.
- [19] C. You, K. Huang, H. Chae, and B.-H. Kim, "Energy-efficient resource allocation for mobile-edge computation offloading," *IEEE Trans. Wireless Commun.*, vol. 16, no. 3, pp. 1397–1411, Mar. 2017.
- [20] M. Zeng, W. Hao, O. A. Dobre, and H. V. Poor, "Delay minimization for massive MIMO assisted mobile edge computing," *IEEE Trans. Veh. Technol.*, vol. 69, no. 6, pp. 6788–6792, Jun. 2020.
- [21] J. Ren, G. Yu, Y. Cai, and Y. He, "Latency optimization for resource allocation in mobile-edge computation offloading," *IEEE Trans. Wireless Commun.*, vol. 17, no. 8, pp. 5506–5519, Aug. 2018.
- [22] W. Zhang, Y. Wen, K. Guan, D. Kilper, H. Luo, and D. O. Wu, "Energy-optimal mobile cloud computing under stochastic wireless channel," *IEEE Trans. Wireless Commun.*, vol. 12, no. 9, pp. 4569–4581, Sep. 2013.
- [23] Y. Wang, M. Sheng, X. Wang, L. Wang, and J. Li, "Mobile-edge computing: Partial computation offloading using dynamic voltage scaling," *IEEE Trans. Commun.*, vol. 64, no. 10, pp. 4268–4282, Oct. 2016.
- [24] T. Q. Dinh, J. Tang, Q. D. La, and T. Q. S. Quek, "Offloading in mobile edge computing: Task allocation and computational frequency scaling," *IEEE Trans. Commun.*, vol. 65, no. 8, pp. 3571–3584, Aug. 2017.
- [25] Y. Mao, J. Zhang, S. H. Song, and K. B. Letaief, "Stochastic joint radio and computational resource management for multi-user mobile-edge computing systems," *IEEE Trans. Wireless Commun.*, vol. 16, no. 9, pp. 5994–6009, Sep. 2017.
- [26] C. Wang, F. R. Yu, C. Liang, Q. Chen, and L. Tang, "Joint computation offloading and interference management in wireless cellular networks with mobile edge computing," *IEEE Trans. Veh. Technol.*, vol. 66, no. 8, pp. 7432–7445, Aug. 2017.

- [27] Q. Li, J. Lei, and J. Lin, “Min-Max latency optimization for multiuser computation offloading in fog-radio access networks,” in *Proc. Int. Conf. on Acoust., Speech and Signal Process. (ICASSP)*, Apr. 2018, pp. 3754–3758.
- [28] T. T. Nguyen, L. Le, and Q. Le-Trung, “Computation offloading in MIMO based mobile edge computing systems under perfect and imperfect CSI estimation,” *IEEE Trans. Services Comput.*, pp. 1–1, Jan. 2019, early access.
- [29] C. Pradhan, A. Li, C. She, Y. Li, and B. Vucetic, “Computation offloading for IoT in C-RAN: Optimization and deep learning,” *IEEE Trans. Commun.*, vol. 68, no. 7, pp. 4565–4579, Jul. 2020.
- [30] Y. Hao, Q. Ni, H. Li, and S. Hou, “Energy-efficient multi-user mobile-edge computation offloading in massive MIMO enabled HetNets,” in *Proc. IEEE Int. Conf. on Commun. (ICC)*, May 2019, pp. 1–6.
- [31] M. Zeng, W. Hao, O. A. Dobre, Z. Ding, and H. V. Poor, “Massive MIMO-assisted mobile edge computing: Exciting possibilities for computation offloading,” *IEEE Veh. Technol. Mag.*, vol. 15, no. 2, pp. 31–38, Jun. 2020.
- [32] Y. Zhao, X. Xu, Y. Su, L. Huang, X. Du, and N. Guizani, “Multi-user MAC protocol for WLANs in MmWave massive MIMO systems with mobile edge computing,” *IEEE Access*, vol. 7, pp. 181 242–181 256, Nov. 2019.
- [33] S. Mukherjee and J. Lee, “Edge computing-enabled cell-free massive MIMO systems,” *IEEE Trans. Wireless Commun.*, vol. 19, no. 4, pp. 2884–2899, Apr. 2020.
- [34] B. R. Marks and G. P. Wright, “A general inner approximation algorithm for nonconvex mathematical programs,” *Operations Research*, vol. 26, no. 4, pp. 681–683, Aug. 1978.
- [35] W. Chen, D. Wang, and K. Li, “Multi-user multi-task computation offloading in green mobile edge cloud computing,” *IEEE Trans. Services Comput.*, vol. 12, no. 5, pp. 726–738, Sep. 2019.
- [36] J. Zheng, Y. Cai, Y. Wu, and X. Shen, “Dynamic computation offloading for mobile cloud computing: A stochastic game-theoretic approach,” *IEEE Transactions on Mobile Computing*, vol. 18, no. 4, pp. 771–786, Apr. 2019.
- [37] S. Boyd and L. Vandenberghe, *Convex optimization*. Cambridge University Press, 2004.
- [38] S. Ulukus and R. Yates, “Stochastic power control for cellular radio systems,” *IEEE Trans. Commun.*, vol. 46, no. 6, pp. 784–798, Jun. 1998.
- [39] R. Yates, “A framework for uplink power control in cellular radio systems,” *IEEE J. Sel. Areas Commun.*, vol. 13, no. 7, pp. 1341–1347, Sep. 1995.
- [40] 3GPP, *Further advancements for E-UTRA physical layer aspects (Release 9)*. 3GPP TS 36.814, Mar. 2017.
- [41] Ö. T. Demir and E. Björnson, “Is channel estimation necessary to select phase-shifts for RIS-assisted massive MIMO?” *CoRR*, vol. abs/2106.09770, 2021. [Online]. Available: <https://arxiv.org/abs/2106.09770>
- [42] MOSEK. ApS, *The MOSEK optimization toolbox for MATLAB manual. Version 9.0.*, 2021. [Online]. Available: <http://docs.mosek.com/9.3/toolbox/index.html>